The massive Klein–Gordon field coupled to a harmonic oscillator at the boundary



2005 J. Phys. A: Math. Gen. 38 7399

(http://iopscience.iop.org/0305-4470/38/33/013)

INSTITUTE OF PHYSICS PUBLISHING JOURNAL OF PHYSICS A: MATHEMATICAL AND GENERAL

J. Phys. A: Math. Gen. **38** (2005) 7399–7418 doi:10.1088/0305-4470/38/33/013

# The massive Klein–Gordon field coupled to a harmonic oscillator at the boundary

**A George**

Department of Mathematics, The University of York, Heslington, York, YO10 5DD, UK

E-mail: ag160@garfield.elte.hu

Received 14 January 2005, in final form 21 June 2005
Published 3 August 2005
Online at stacks.iop.org/JPhysA/38/7399

**Abstract**

We consider the massive Klein–Gordon field on the half line with and without a Robin boundary potential. The field is coupled at the boundary to a harmonic oscillator. We solve the system classically and observe the existence of classical boundary bound states in some regions of the parameter space. The system is then quantized, the quantum reflection matrix and reflection cross section are calculated. Resonances and Ramsauer–Townsend effects are observed in the cross section. The pole structure of the reflection matrix is discussed.

PACS numbers: 11.10.−z, 03.65.Pm

The study of quantum fields with boundaries has been the subject of much work in recent years. There have been two main methods used to study such systems; integrable boundary field theory (see, for example, [1, 2]) and boundary perturbation theory (see [3], and references there in). Both approaches have focused on situations where the boundary is a non-dynamic object that does not contain its own internal degrees of freedom. Recently some studies have been conducted on the coupling of both classical and quantum fields to boundaries, or impurities, containing additional degrees of freedom, for instance, dynamic boundary conditions have been studied for the integrable sine-Gordon [4–7], supersymmetric sine-Gordon [8], free fermion fields [9] and several authors have studied the coupling of the massless Klein–Gordon field to oscillators, e.g. [10–13]. These models can be used in the study of such physical systems as excited atoms in cavities and quantum wires containing impurities. Boundary degrees of freedom are also of interest in the study of brane–bulk interactions in braneworld universes, see, for example, [14].

In this paper we consider another system consisting of a field with a dynamic boundary. This 'toy model' consists of a massive Klein–Gordon field in 1+1 dimensions restricted to the left half line by a boundary. The field is linearly coupled to a harmonic oscillator at the boundary thus introducing the additional degrees of freedom. Although this model is entirely linear, and may therefore appear trivial on first inspection, we will see it possesses several

  

interesting, non-obvious features. The full analysis of these features, which we are able to undertake due to its linear nature, will help in the interpretation of similar effects in other non-integrable models and in systems where perturbative methods cannot be applied.

In section 1 we review previous results for the massive Klein–Gordon field with the Robin boundary condition. In section 2 we consider the massive Klein–Gordon field on the halfline coupled to a harmonic oscillator at the boundary with a Robin boundary potential. The system is solved in the classical regime and boundary bound states are observed in some regions of the parameter space. We show that the classical solutions of the system can be decomposed into independent modes of oscillation. We observe that the existence of boundary bound states combined with the requirement that the Hamiltonian be bounded below restricts the possible values of the parameters of the theory. We then quantize the field directly from the classical solutions expressed as a superposition of the independent modes and find the quantum reflection matrices of the systems from the two point function of the field. From the reflection matrix we calculate the reflection cross section, and resonances and Ramsauer–Townsend effects are observed for some ranges of the parameter spaces. We discuss the pole structure of the quantum reflection matrices. At the end of section 2 we consider the special case when the Robin boundary potential is absent. Section 3 contains a discussion on the main results of this paper, and possible directions for future work in the area.

## 1. The massive Klein–Gordon field with a Robin boundary

In this section we consider an example of an exactly solvable boundary field theory, the massive Klein–Gordon field on the left half line with a Robin boundary potential. This system has been studied previously, see, for example, [3, 15].

### *1.1. Classical system*

The Hamiltonian for this system is given by

$$H = \int_{-\infty}^{0} \left( \frac{1}{2}\pi(x,t)^2 + \frac{1}{2}(\partial_x \phi(x,t))^2 + \frac{1}{2}m^2\phi(x,t)^2 \right) \mathrm{d}x + \frac{1}{2}\lambda\phi(0,t)^2, \tag{1}$$

where $\phi(x,t)$ and $\pi(x,t)$ are the field and its conjugate momentum which have the Poisson bracket relations $\{\phi(x,t), \pi(y,t)\} = \delta(x-y)$. The boundary coupling parameter $\lambda$ is assumed to be real.

From (1) we find Hamilton's equations for the system[1],

$$\partial_t \phi(x,t) = \{\phi(x,t), H\} = \pi(x,t), \tag{2}$$

$$\partial_t \pi(x,t) = \{\pi(x,t), H\} = \partial_x^2 \phi(x,t) - m^2\phi(x,t) - \delta(x)(\partial_x\phi(0,t) + \lambda\phi(0,t)). \tag{3}$$

From (2) and (3) we find the Robin boundary condition by requiring that $\pi(x,t)$ be continuous at the origin,

$$\partial_x \phi(0,t) = -\lambda\phi(0,t). \tag{4}$$

From Hamilton's equations (2) and (3) and the boundary condition (4) we recover the usual equation of motion for the massive Klein–Gordon field,

$$\partial_t^2 \phi(x,t) = \partial_x^2 \phi(x,t) - m^2\phi(x,t). \tag{5}$$

[1] Here and throughout this paper the notation $\partial_x\phi(0,t)$ should be read as the derivative with respect to $x$ of $\phi(x,t)$ evaluated at $x = 0$, i.e. a shortened notation for $\partial_x\phi(x,t)|_{x=0}$.

The equation of motion (5) and boundary condition (4) are satisfied by the 'bulk' solutions,

$$\phi(x,t) = \int_0^\infty \left(\cos(\rho x) - \frac{\lambda}{\rho}\sin(\rho x)\right)\left(a(\rho)\cos(\omega_\rho t) + \frac{b(\rho)}{\omega_\rho}\sin(\omega_\rho t)\right)\mathrm{d}\rho, \tag{6}$$

where $a(\rho)$ and $b(\rho)$ are real functions of $\rho$ and $\omega_\rho = \sqrt{m^2+\rho^2}$.

As well as the 'bulk' solutions there can exist square integrable boundary bound state solutions. Such solutions can be found by allowing the momentum, $\rho$, of the bulk solutions, given in this case by (6), to take imaginary values, $\rho = \mathrm{i}\varrho$. Because the bulk solutions satisfy the boundary condition (4) and the equation of motion of the bulk field (5) the imaginary momentum solutions will also satisfy these equations. However, such solutions will, generally, cause the field to diverge as $x \to -\infty$ and so must be discarded[2]. However, for special values of $\varrho$ the divergence of the field arising from terms proportional to $\cosh(\varrho x)$ and that arising from terms proportional to $\sinh(\varrho x)$ cancel out on the left half line. At such values of $\varrho$ there exists a valid boundary bound state. Such a valid boundary bound state exists for the Robin boundary at $\varrho = -\lambda$ provided $\lambda$ is negative[3]. The boundary bound state solution is then

$$\phi(x,t) = \mathrm{e}^{\varrho x}\left(a_\varrho\cos(\omega_\varrho t) + \frac{b_\varrho}{\omega_\varrho}\sin(\omega_\varrho t)\right), \tag{7}$$

where $a_\varrho$ and $b_\varrho$ are real amplitudes and $\omega_\varrho = \sqrt{m^2-\varrho^2}$. Note that there is only a boundary bound state for negative values of $\lambda$, i.e., when the contribution of the boundary term to the Hamiltonian (1) is negative. Such boundaries are called attractive, those for which the contribution of the boundary term to the Hamiltonian is positive are called repulsive boundaries. Repulsive boundaries cannot support boundary bound states of this form. Also note that when $\varrho^2 > m^2$ the value of $\omega_\varrho$ becomes imaginary and the boundary bound state solution diverges as $t \to \pm\infty$. The most general solution for the Robin boundary is formed by adding the bulk solutions to the boundary bound state solution, if one exists.

We can now try substituting these solutions into the Hamiltonian (1). Let us first assume that $\lambda$ is positive, i.e. the boundary is repulsive and there exists no boundary bound state. Taking each term of the Hamiltonian in turn at $t = 0$, substituting the expressions for the bulk solutions (6) we find that

$$H = \int_0^\infty \frac{1}{2}\tilde{b}(\rho)^2 + \frac{1}{2}\omega_\rho^2\tilde{a}(\rho)^2\,\mathrm{d}\rho, \tag{8}$$

where

$$\tilde{a}(\rho) := \sqrt{\frac{\pi}{2}}a(\rho)\left(1+\frac{\lambda^2}{\rho^2}\right)^{1/2}, \tag{9}$$

$$\tilde{b}(\rho) := \sqrt{\frac{\pi}{2}}b(\rho)\left(1+\frac{\lambda^2}{\rho^2}\right)^{1/2}. \tag{10}$$

When $\lambda$ is negative we must also include the boundary bound state solution when we are substituting into the Hamiltonian (1). This results in an additional term appearing in (8) corresponding to the energy contribution of the additional mode. The Hamiltonian for the attractive Robin boundary is

$$H = \int_0^\infty \frac{1}{2}\tilde{b}(\rho)^2 + \frac{1}{2}\omega_\rho^2\tilde{a}(\rho)^2\,\mathrm{d}\rho + \frac{1}{2}\tilde{b}_\varrho^2 + \frac{1}{2}\omega_\varrho^2\tilde{a}_\varrho^2, \tag{11}$$

[2] The field is required to be bounded over its domain, thus solutions which diverge on the left half line must be discarded.

[3] If $\lambda$ is positive there is no solution which decays on the left half line instead there is a solution which exponentially grows as $x \to -\infty$ which must be rejected.

where $\tilde{a}(\rho)$ and $\tilde{b}(\rho)$ are given by (9) and (10) and

$$\tilde{a}_\varrho := \frac{a_\varrho}{(2|\lambda|)^{1/2}}, \qquad \tilde{b}_\varrho := \frac{b_\varrho}{(2|\lambda|)^{1/2}}.$$

Note that if $\lambda^2 > m^2$ then $\omega_\varrho^2$ is negative. This would mean that the Hamiltonian (11) would not be bounded below and thus be unphysical. It is therefore a requirement on the parameters of the theory that $\lambda^2 \leqslant m^2$ for the attractive Robin boundary, as the repulsive boundary has no such bound state there does not exist an equivalent condition, the Hamiltonian is always bounded below.

### *1.2. Quantum system*

As both the Hamiltonian for the repulsive (8) and the attractive Robin boundaries (11) are now written as an infinite sum of harmonic oscillators we can quantize the field in the canonical fashion. For each mode we have a creation and annihilation operator,

$$\alpha^\dagger(\rho) := \sqrt{\frac{\omega_\rho}{2}}\left(\tilde{a}(\rho) - \mathrm{i}\frac{\tilde{b}(\rho)}{\omega_\rho}\right), \qquad \alpha(\rho) := \sqrt{\frac{\omega_\rho}{2}}\left(\tilde{a}(\rho) + \mathrm{i}\frac{\tilde{b}(\rho)}{\omega_\rho}\right),$$

$$\alpha_\varrho^\dagger := \sqrt{\frac{\omega_\varrho}{2}}\left(\tilde{a}_\varrho - \mathrm{i}\frac{\tilde{b}_\varrho}{\omega_\varrho}\right), \qquad \alpha_\varrho := \sqrt{\frac{\omega_\varrho}{2}}\left(\tilde{a}_\varrho + \mathrm{i}\frac{\tilde{b}_\varrho}{\omega_\varrho}\right).$$

The 'bulk' creation operators, $\alpha^\dagger(\rho)$, act on the vacuum to produce bulk particles of the field. These particles are located far to the left of the boundary at $t = -\infty$ with momentum $p = \rho$ they propagate to the boundary from which they reflect. At $t = \infty$ these particles are once again located far to the left of the boundary and have momentum $p = -\rho$. The creation operator associated with the boundary bound state, $\alpha_\varrho^\dagger$, acts on the vacuum to create a particle of the field with energy lower than that of a stationary bulk particle, this particle is trapped close to the boundary at all times.

The one-particle quantum reflection matrix, or $R$-matrix, for the massive Klein–Gordon field with a linear boundary can be found directly from the two point function of the quantized field,

$$\begin{aligned}\langle 0|\phi(x_2,t_2)\phi(x_1,t_1)|0\rangle = &\int_{-\infty}^{\infty} \frac{1}{4\pi\omega_p}\,\mathrm{e}^{-\mathrm{i}p(x_2-x_1)}\,\mathrm{e}^{-\mathrm{i}\omega_p(t_2-t_1)}\,\mathrm{d}p \\ &+ \int_{-\infty}^{\infty} \frac{1}{4\pi\omega_p} R(p)\,\mathrm{e}^{-\mathrm{i}p(x_2+x_1)}\,\mathrm{e}^{-\mathrm{i}\omega_p(t_2-t_1)}\,\mathrm{d}p \\ &+ \text{boundary bound state contributions.}\end{aligned} \tag{12}$$

The first integral on the right-hand side of (12) is the standard two point function of the Klein–Gordon field. This corresponds to a particle propagating between the space time points $(x_1, t_1)$ and $(x_2, t_2)$. The second integral corresponds to a particle propagating between the same two points via the boundary where it is reflected and picks up the momentum-dependent amplitude $R(p)$, which is equivalent to the $R$-matrix found using any other commonly used definitions, see [16]. The third term on the right-hand side of (12) arises from any boundary bound states of the system, such contributions will fall off to zero as $x_1 \to -\infty$ and $x_2 \to -\infty$ due to the localization of the boundary bound state particles close to the boundary.

Using these creation and annihilation operators, the definition of the quantum reflection matrix (12) and the expressions for the general bulk solutions of the field (6) it is simple to calculate the $R$-matrix for the Robin boundary to be

$$R(p) = \frac{p - \mathrm{i}\lambda}{p + \mathrm{i}\lambda}. \tag{13}$$

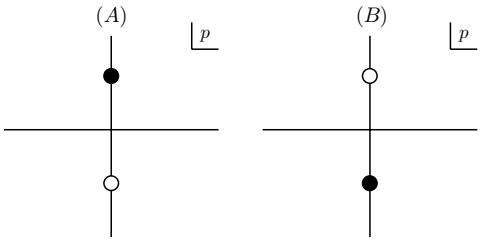


**Figure 1.** The analytic structure of the quantum reflection matrix for the Robin boundary for (*A*) $\lambda < 0$ and (*B*) $\lambda > 0$.

Let us consider the analytic structure of (13). There is always a single pole located at $p = -\mathrm{i}\lambda$. When $\lambda$ is negative this pole appears in the upper complex half plane as shown in figure 1(*A*) where the black circle indicates the pole and the white circle indicates a node. The pole occurs at the same value of imaginary momentum for which we have observed a classical boundary bound state. The interpretation of this pole is clear, it corresponds to the existence of a quantum boundary bound state which is equivalent to the classical boundary bound state. However, when $\lambda$ is positive, and the pole appears in the lower complex half plane as shown in figure 1(*B*), there is no classical boundary state to which the pole can correspond and the pole does not correspond to a quantum state of the system either.

## 2. Coupling the massive Klein–Gordon field to a boundary oscillator in the presence of a Robin potential

In this section we consider the massive Klein–Gordon field in 1+1 dimensions restricted to the left half line with a Robin boundary potential. In addition the field is linearly coupled to a harmonic oscillator at the boundary thus introducing an additional degrees of freedom. This preserves the linear, and thus exactly solvable, nature of the theory but introduces new and interesting features into the reflection cross section.

### *2.1. Classical system*

The Hamiltonian for this system is

$$H = \int_{-\infty}^{0} \left( \frac{1}{2}\pi(x,t)^2 + \frac{1}{2}(\partial_x \phi(x,t))^2 + \frac{1}{2}m^2\phi(x,t)^2 \right) \mathrm{d}x + \frac{1}{2}\lambda\phi(0,t)^2 + \beta\phi(0,t)q(t) + \frac{1}{2}\mu^2 q(t)^2 + \frac{1}{2}p(t)^2, \tag{14}$$

where $\pi(x,t)$ is the conjugate momentum to the field $\phi(x,t)$, and $p(t)$ is the conjugate momentum to the oscillator $q(t)$. These have the usual equal time Poisson bracket relations, $\{\phi(x,t), \pi(y,t)\} = \delta(x-y)$, $\{q(t),\ p(t)\} = 1$, all other brackets are zero. The parameters of the theory are the mass of the field, $m$, the Robin boundary coupling parameter, $\lambda$, the boundary oscillator coupling parameter, $\beta$ and the natural frequency of the boundary oscillator, $\mu$. In natural units[4] these parameters have dimensions $[m] = [\mu] = [\lambda] = [M]$, $[\beta] = [M^{3/2}]$ and for the oscillator $[q(t)] = [M^{-1/2}]$ and $[p(t)] = [M^{1/2}]$. The parameters $m$, $\mu$, $\lambda$ and $\beta$ are assumed to be real and $m$ and $\mu$ are taken to be positive.

[4] Setting $c = \hbar = 1$, gives relations between the dimensions, $[M] = [L^{-1}] = [T^{-1}]$.

Hamilton's equations for the field and oscillator are

$$\partial_t \phi(x,t) = \{\phi(x,t), H\} = \pi(x,t), \tag{15}$$

$$\partial_t \pi(x,t) = \{\pi(x,t), H\} = \partial_x^2 \phi(x,t) - m^2\phi(x,t) - \delta(x)(\partial_x \phi(0,t) + \lambda\phi(0,t) + \beta q(t)), \tag{16}$$

$$\partial_t q(t) = \{q(t), H\} = p(t), \tag{17}$$

$$\partial_t p(t) = \{p(t), H\} = -\beta\phi(0,t) - \mu^2 q(t). \tag{18}$$

From (16) we find the boundary condition necessary for $\pi(x,t)$ to be continuous to be

$$\partial_x \phi(0,t) = -\lambda\phi(0,t) - \beta q(t). \tag{19}$$

Combining the boundary condition (19) and Hamilton's equations (15) and (16) we recover the equation of motion for the Klein–Gordon field

$$\partial_t^2 \phi(x,t) = \partial_x^2 \phi(x,t) - m^2\phi(x,t). \tag{20}$$

Similarly we find the equation of motion for the boundary oscillator from Hamilton's equations (17) and (18) to be

$$\partial_t^2 q(t) = -\beta\phi(0,t) - \mu^2 q(t). \tag{21}$$

The equations of motion (20) and (21) and boundary condition (19) are satisfied by the bulk solutions,

$$\phi(x,t) = \int_0^\infty (\rho(\rho^2 - \mu^2 + m^2)\cos(\rho x) - (\lambda(\rho^2 - \mu^2 + m^2) + \beta^2)\sin(\rho x)) \times (a(\rho)\cos(\omega_\rho t) + b(\rho)\sin(\omega_\rho t)), \tag{22}$$

$$q(t) = \int_0^\infty \beta\rho(a(\rho)\cos(\omega_\rho t) + b(\rho)\sin(\omega_\rho t))\,\mathrm{d}\rho, \tag{23}$$

where $\omega_\rho = \sqrt{m^2 + \rho^2}$ and $a(\rho)$ and $b(\rho)$ are real functions of $\rho$.

These solutions have several interesting features. For large $\lambda$ or $\beta$ the solutions for the field become equivalent, after a rescaling of $a(\rho)$ and $b(\rho)$, to solutions for the Dirichlet boundary condition and for small $\lambda$ and $\beta$ the field solutions become the same as for a Neumann boundary. These qualitative features of the bulk solutions are shared by the solutions for the Robin boundary condition discussed in section 1, this behaviour is said to èxtrapolate between the Dirichlet and Neumann boundary conditions'. The solutions for the dynamic boundary (22) and (23) contain additional interesting features. In the region of the parameter space where $\mu > m$ there exists a value of $\rho$, $\rho = \sqrt{\mu^2 - m^2}$ at which for any value of $\beta$ and $\lambda$ the solution, for this one mode, becomes proportional to $\sin(\rho x)$, this can be interpreted as a resonance effect, at this value of $\rho$ the field is oscillating with frequency $\omega_\rho = \mu$, the natural frequency of the boundary oscillator. A second feature in the solutions not previously observed for just the Robin boundary potential is that when $\lambda\rho^2 = \lambda(\mu^2 - m^2) - \beta^2$ the single mode solution becomes proportional to $\cos(\rho x)$. In the next section we will return to these features when we consider the reflection cross section of this boundary.

In addition to the spatially oscillating 'bulk' solutions there exist square integrable 'boundary bound state' solutions found from the bulk solutions by allowing the parameter $\rho$ to take imaginary values $\rho = \mathrm{i}\varrho$ and requiring that the divergence of the field on the left half line arising from the terms proportional to $\cosh(\varrho x)$ and $\sinh(\varrho x)$ cancel. These solutions have the form

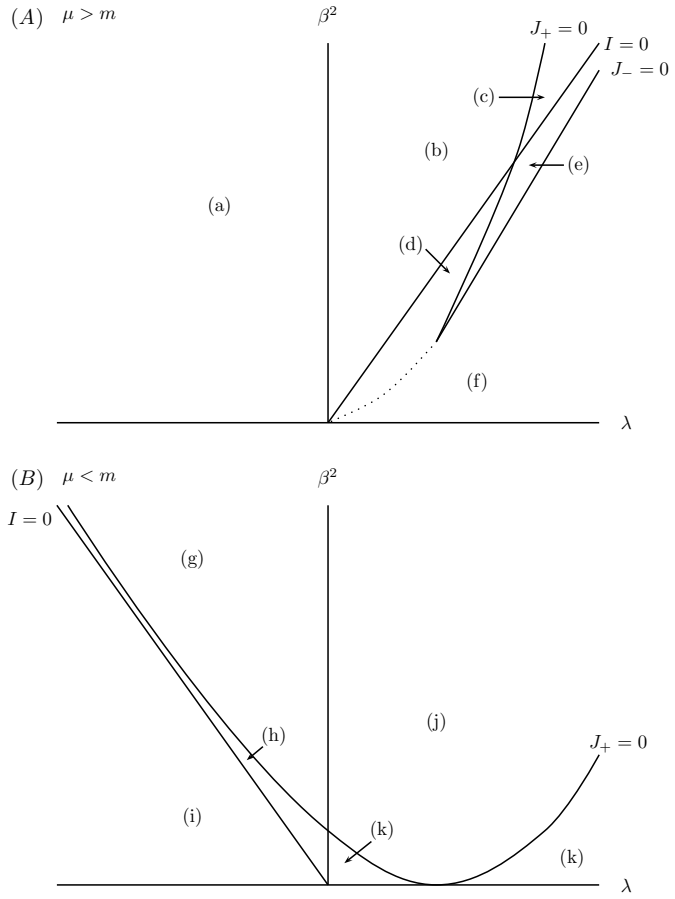


**Figure 2.** The various regions of the parameter space of the dynamic boundary with Robin potential theory for (*A*) $\mu > m$ and (*B*) $\mu < m$.

$$\phi(x,t) = \mathrm{e}^{\varrho x}(a_\varrho \cos(\omega_\varrho t) + b_\varrho \sin(\omega_\varrho t)), \tag{24}$$

$$q(t) = -\frac{\varrho + \lambda}{\beta}(a_\varrho \cos(\omega_\varrho t) + b_\varrho \sin(\omega_\varrho t)), \tag{25}$$

where $\omega_\varrho = \sqrt{m^2 - \varrho^2}$, $a_\varrho$ and $b_\varrho$ are real amplitudes and $\varrho$ is a positive real solution of

$$\varrho^3 + \lambda\varrho^2 + (\mu^2 - m^2)\varrho + \lambda(\mu^2 - m^2) - \beta^2 = 0. \tag{26}$$

We can split the parameter space of the theory into regions, using the planes

- $\mu^2 - m^2 = 0$,
- $\lambda = 0$,
- $I = \lambda(\mu^2 - m^2) - \beta^2 = 0$,
- $J_\pm = \frac{2}{3}\lambda(\mu^2 - m^2) + \frac{2}{27}\lambda^3 \pm \frac{2}{27}(\lambda^2 - 3(\mu^2 - m^2))^{3/2} - \beta^2 = 0$.

The value of $I$ is the value of the cubic $\varrho^3 + \lambda\varrho^2 + (\mu^2 - m^2)\varrho + \lambda(\mu^2 - m^2) - \beta^2$ at $\varrho = 0$, $J_+$ is the value of the cubic at the local maximum of the function and $J_-$ is the value of the cubic at the local minimum. If $\lambda^2 < 3(\mu^2 - m^2)$ there are no stationary points and $J_\pm$ take complex values. When this occurs we use the real part of $J_\pm = 0$ as the boundary between regions. Figure 2 shows how the parameter space of the theory is divided up by these planes.

It is simple to find how many real solutions of (26) exist in each of these regions. For $\mu > m$ there is a single positive real solution if $I < 0$ which corresponds to regions (a), (b) and (c) in figure 2(*A*), if $J_+ < 0$, i.e. region (c), there are also two negative real solutions to (26). If $\mu > m$ and $I > 0$ then there are no positive real solutions, but there is a single real negative solution in regions (d) and (f ) and three negative solutions in region (e). When $\mu < m$ there is a single positive solution to (26) if $I < 0$, i.e. in regions (g), (h), ( j) and (k) of figure 2(*B*). In regions (h) and (k) there are also two negative real solutions. When $\mu < m$ and $I > 0$, i.e. in region (i) there are two positive real solutions and one negative real solution. As only positive real solutions of (26) correspond to classical boundary bound state solutions this means there exist one such solution in regions (a), (b), (c), (g), (h), ( j) and (k). There are no boundary bound states in regions (d), (e) and (f ) and there are two classical boundary bound state solutions in region (i).

For (24) and (25) to describe time oscillatory states $\varrho$ must be less than $m$. Using (26) it is possible to express this requirement as an inequality between the parameters of the model,

$$\frac{\beta^2}{\mu^2} - \lambda \leqslant m. \tag{27}$$

If this condition is satisfied the boundary bound states of the system are time oscillatory, otherwise they are solutions in which the field diverges as $t \to \pm\infty$.

Classical boundary bound state solutions for the Klein–Gordon field have previously been observed for the Robin boundary, as discussed in section 1, where the equivalent condition to (47) for the bound state to be oscillatory is $-\lambda \leqslant m$. It is worth noting that the bound state only exists for the attractive Robin boundary, i.e. $\lambda < 0$. If $\lambda > 0$ then the Robin boundary is repulsive and no bound state exists.

We will now show that the solutions (22)–(25) can be written as a superposition of orthogonal-independent modes of oscillation. Let us define

$$\tilde{a}(\rho) := \sqrt{\frac{\pi}{2}} a(\rho)(\rho^2(\rho^2 - \mu^2 + m^2)^2 + (\lambda(\rho^2 - \mu^2 + m^2) + \beta^2)^2)^{1/2}, \tag{28}$$

$$\tilde{b}(\rho) := \sqrt{\frac{\pi}{2}} b(\rho)\omega_\rho(\rho^2(\rho^2 - \mu^2 + m^2)^2 + (\lambda(\rho^2 - \mu^2 + m^2) + \beta^2)^2)^{1/2}, \tag{29}$$

$$\tilde{a}_\varrho := a_\varrho \left(\frac{\beta^2 + 2\rho(\rho+\lambda)^2}{2\beta^2\rho}\right)^{1/2}, \tag{30}$$

$$\tilde{b}_\varrho := b_\varrho\omega_\varrho \left(\frac{\beta^2 + 2\rho(\rho+\lambda)^2}{2\beta^2\rho}\right)^{1/2}, \tag{31}$$

$$\psi(\rho, x) := \frac{\rho(\rho^2 - \mu^2 + m^2)\cos(\rho x) - (\lambda(\rho^2 - \mu^2 + m^2 + \beta^2)\sin(\rho x)}{\sqrt{\frac{\pi}{2}}(\rho^2(\rho^2 - \mu^2 + m^2)^2 + (\lambda(\rho^2 - \mu^2 + m^2) + \beta^2)^2)^{1/2}}, \tag{32}$$

$$\chi(\rho) := \frac{\beta\rho}{\sqrt{\frac{\pi}{2}}((\rho^2(\rho^2 - \mu^2 + m^2)^2 + (\lambda(\rho^2 - \mu^2 + m^2) + \beta^2)^2)^{1/2}}, \tag{33}$$

$$\psi_\varrho(x) := \mathrm{e}^{\varrho x}\left(\frac{2\beta^2\rho}{\beta^2 + 2\rho(\rho+\lambda)^2}\right)^{1/2}, \tag{34}$$

$$\chi_\varrho := -\frac{\rho+\lambda}{\beta}\left(\frac{2\beta^2\rho}{\beta^2 + 2\rho(\rho+\lambda)^2}\right)^{1/2}. \tag{35}$$

We can now write the general solutions in terms of the definitions (28)–(35) as

$$\phi(x,t) = \int_0^\infty \left(\tilde{a}(\rho)\psi(\rho,x)\cos(\omega_\rho t) + \frac{\tilde{b}(\rho)}{\omega_\rho}\psi(\rho,x)\sin(\omega_\rho t)\right)\mathrm{d}\rho + \sum_\varrho \left(\tilde{a}_\varrho\psi_\varrho(x)\cos(\omega_\varrho t) + \frac{\tilde{b}_\varrho}{\omega_\varrho}\psi_\varrho(x)\sin(\omega_\varrho t)\right), \tag{36}$$

$$q(t) = \int_0^\infty \left(\tilde{a}(\rho)\chi(\rho)\cos(\omega_\rho t) + \frac{\tilde{b}(\rho)}{\omega_\rho}\chi(\rho)\sin(\omega_\rho t)\right)\mathrm{d}\rho + \sum_\varrho \left(\tilde{a}_\varrho\chi_\varrho\cos(\omega_\varrho t) + \frac{\tilde{b}_\varrho}{\omega_\varrho}\chi_\varrho\sin(\omega_\varrho t)\right). \tag{37}$$

The sum in (36) and (37) runs over all positive real roots of (26). The functions (32)–(35) form an orthonormal set over the half line plus the oscillator,

$$\int_0^\infty \psi(\rho_1,x)\psi(\rho_2,x)\,\mathrm{d}x + \chi(\rho_1)\chi(\rho_2) = \delta(\rho_1-\rho_2), \tag{38}$$

$$\int_0^\infty \psi_\varrho(x)\psi(\rho,x)\,\mathrm{d}x + \chi_\varrho\chi(\rho) = 0, \tag{39}$$

$$\int_0^\infty \psi_{\varrho_1}(x)\psi_{\varrho_2}(x)\,\mathrm{d}x + \chi_{\varrho_1}\chi_{\varrho_2} = \delta_{\varrho_1\varrho_2}. \tag{40}$$

Relation (38) holds as $\rho$ is always positive, (39) requires that $\varrho$ is a root of (26) and (40) uses the relations between roots of a cubic equation[5]. By substituting the general solutions (36) and (37) into the Hamiltonian (14) and applying the othoganality relations (38)–(40) we can rewrite the Hamiltonian as an infinite sum of independent harmonic oscillators each corresponding to one mode of oscillation of the field[6],

$$H = \frac{1}{2}\int_0^\infty \tilde{b}(\rho)^2 + \omega_\rho^2\tilde{a}(\rho)^2\,\mathrm{d}\rho + \frac{1}{2}\sum_\varrho \tilde{b}_\varrho^2 + \omega_\varrho^2\tilde{a}_\varrho^2. \tag{41}$$

Note that the Hamiltonian (41) is bounded below only if $\omega_\varrho$ is real, i.e. if all the boundary bound state modes are oscillatory, which occurs only when (27) is satisfied. Thus we must require that the condition (27) be satisfied to have a physical system.

### 2.2. *Quantum system*

By using the definitions (28)–(35) we have described the general classical solutions for the field as the linear superposition of independent modes of oscillation. The Hamiltonian in this basis can be written as a sum over an infinite number of harmonic oscillators each corresponding to one of the modes of oscillation (41). It is now simple to quantize the system, by analogy to the quantization of the unbounded field we can define creation and annihilation operators,

$$\alpha(\rho) := \sqrt{\frac{\omega_\rho}{2}}\left(\tilde{a}(\rho) - \mathrm{i}\frac{\tilde{b}(\rho)}{\omega_\rho}\right), \qquad \alpha_\varrho := \sqrt{\frac{\omega_\varrho}{2}}\left(\tilde{a}_\varrho - \mathrm{i}\frac{\tilde{b}_\varrho}{\omega_\varrho}\right),$$
$$\alpha^\dagger(\rho) := \sqrt{\frac{\omega_\rho}{2}}\left(\tilde{a}(\rho) + \mathrm{i}\frac{\tilde{b}(\rho)}{\omega_\rho}\right), \qquad \alpha_\varrho^\dagger := \sqrt{\frac{\omega_\varrho}{2}}\left(\tilde{a}_\varrho + \mathrm{i}\frac{\tilde{b}_\varrho}{\omega_\varrho}\right).$$

[5] Let the roots of the cubic $z^3 + c_2z^2 + c_1z + c_0$ be $z_1, z_2$ and $z_3$. These roots satisfy the relations $z_1z_2z_3 = -c_0$, $z_1z_2 + z_1z_3 + z_2z_3 = c_1$ and $z_1 + z_2 + z_3 = -c_2$.

[6] That is the integral over all bulk modes plus the sum over the finite number of boundstate modes.

Here there is one pair of creation annihilation operators for each allowed boundary bound state. The operators have the usual commutation relations for creation and annihilation operators, $[\alpha(\rho_1), \alpha^\dagger(\rho_2)] = \delta(\rho_1 - \rho_2)$, $\left[\alpha_\varrho, \alpha_\varrho^\dagger\right] = 1$, and $\left[\alpha(\rho), \alpha_\varrho^\dagger\right] = [\alpha_\varrho, \alpha^\dagger(\rho)] = 0$.

Using these operators we can construct a Fock space, let the vacuum, $|0\rangle$, be the state which vanishes when acted on by any of the annihilation operators, $\alpha(\rho)|0\rangle = 0$, $\alpha_\varrho|0\rangle = 0$. The one-particle 'bulk' states are created by the action of $\alpha^\dagger(\rho)$ on the vacuum, $\alpha^\dagger(\rho)|0\rangle = |\rho\rangle$, and one particle boundary states are created by the action of $\alpha_\varrho^\dagger$ on the vacuum, $\alpha_\varrho^\dagger|0\rangle = |\varrho\rangle$. The one-particle bulk states, $|\rho\rangle$, represent a particle of mass $m$ that at $t = -\infty$ is located far to the left of the boundary and is travelling with momentum $p = \rho$ towards the boundary. At time $t = \infty$ this particle is again located far to the left but is travelling away from the boundary with momentum $p = -\rho$. At some finite time the particle has approached and reflected from the boundary. Boundary states, $|\varrho\rangle$, represent particles which are located close to the boundary at all times. Annihilation operators act on the one-particle states to return the vacuum or zero, $\alpha(\rho_1)|\rho_2\rangle = \delta(\rho_1 - \rho_2)|0\rangle$, $\alpha_{\varrho_1}|\varrho_2\rangle = \delta_{\varrho_1\varrho_2}|0\rangle$. Multi-particle states can be constructed from the action of several creation operators on the vacuum. We can define the number operator for both the bulk particle states, $N(\rho) := \alpha^\dagger(\rho)\alpha(\rho)$, and for the boundary states, $N_\varrho := \alpha_\varrho^\dagger\alpha_\varrho$, from which we can construct the renormalized Hamiltonian,

$$\hat{H} := \int_0^\infty \omega_\rho N(\rho)\,\mathrm{d}\rho + \sum_\varrho \omega_\varrho N_\varrho. \tag{42}$$

This is equivalent to the classical Hamiltonian (41) up to a constant infinite term. From equation (42) and the definition of $\omega_\rho$ we see that the renormalized Hamiltonian is Hermitian if and only if $\omega_\varrho$ is real. This is the same requirement as that for the classical boundary bound states to be oscillatory in time. It has already been shown that this condition is equivalent to equation (27). Thus provided that the condition (27) between the parameters of the model holds the renormalized Hamiltonian (42) will be a Hermitian operator. If (47) does not hold the theory has an unstable vacuum and cannot be quantized.

From the general solution for the field (36) and the definition (12) we find the reflection matrix to be

$$R(p) = \frac{p(p^2 - \mu^2 + m^2) - \mathrm{i}(\lambda(p^2 - \mu^2 + m^2) + \beta^2)}{p(p^2 - \mu^2 + m^2) + \mathrm{i}(\lambda(p^2 - \mu^2 + m^2) + \beta^2)}. \tag{43}$$

Note that $R(p)$ is unitary $R(p)^*R(p) = 1$ and that as the parameter $p$ is the momentum of incoming particles and as the boundary defines the right most limit of the field all incoming particles will have positive momentum, thus it is sufficient for us to consider just these values of $p$.

The reflection matrix (43) has three poles corresponding to the three complex roots of (26). These poles either occur at positive, purely imaginary, values of momentum ($p = \mathrm{i}\varrho$) in which case they correspond to the bound state of the system, or they occur at values of momentum in the lower half complex plane. To help interpret these poles we define the total reflection cross section by analogy with the optical theorem for bulk scattering,

$$\sigma_{\mathrm{tot}}(\rho) \propto \frac{1}{2}\Im(Q(\rho)) = \frac{(\lambda(\rho^2 - \mu^2 + m^2) + \beta^2)^2}{\rho^2(\rho^2 - \mu^2 + m^2)^2 + (\lambda(\rho^2 - \mu^2 + m^2) + \beta^2)^2}, \tag{44}$$

where $Q(\rho) = (-\mathrm{i})(R(\rho) - 1)$ and $\Im(Q(\rho))$ indicates that we are taking the imaginary part of $Q(\rho)$. The total reflection cross section $\sigma_{\mathrm{tot}}(\rho)$, measures the probability that, during the reflection process, the reflecting particle in state $|\rho\rangle$ is scattered into some intermediate state, $|\varsigma\rangle$, which then decays back into the original state[7]. Figure 3(*A*) shows the shape of $\sigma_{\mathrm{tot}}$ for

[7] The total cross section $\sigma_{\mathrm{tot}}$ here does not have a direct clear interpretation due to quantum mechanical interference between scattering and non-scattering terms, we pursue this interpretation through analogy with the bulk case.

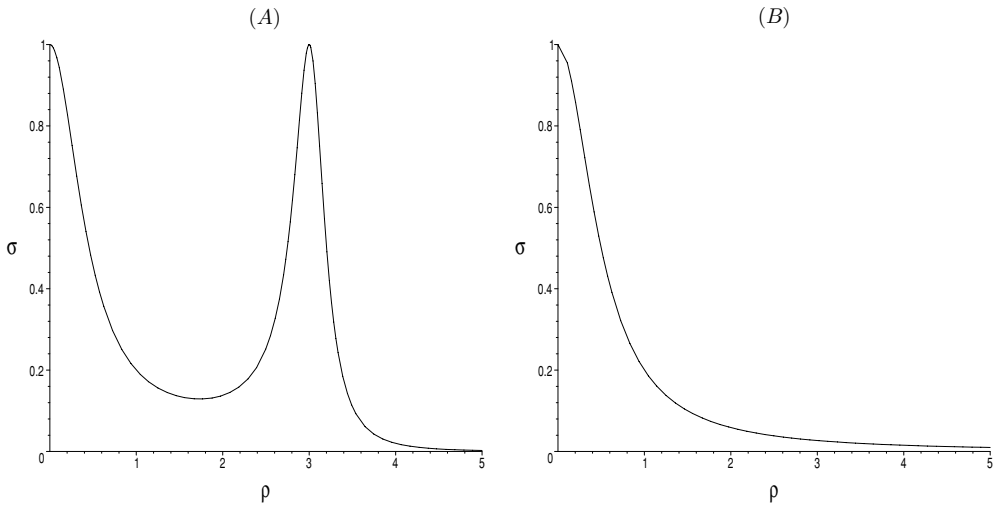


**Figure 3.** The total reflection cross sections of ($A$) the dynamic boundary with $m = 4,\ \mu = 5,$ $\beta = 2,\ \lambda = 0$ and ($B$) the repulsive Robin boundary with $\lambda = \frac{1}{2}$.

the dynamic boundary in the region of the parameter space where $\mu > m$, for the special case when $\lambda = 0$. For comparison figure 3($B$) shows the shape of the total reflection cross section of the Robin boundary. Both reflection cross sections exhibit a background effect where, for low momentum particles, the cross section increases arising from the attraction or repulsion of the boundary to the scattering bulk particles.

The reflection cross section (44) has two other important features, the first is a resonance peak around $\rho = \sqrt{\mu^2 - m^2}$ where the cross section is large the second is a minimum where the cross section falls to zero at $\lambda\rho^2 = \lambda(\mu^2 - m^2) - \beta^2$. These two features correspond to when the classical solutions are proportional to $\sin(\rho x)$ and $\cos(\rho x)$, respectively. Note that figure 3($A$) also exhibits a resonance peak but no minimum, we will discuss this special case in a later section. The resonance is only observable in the reflection cross section when $\mu > m$ as $\rho$ is positive and real for the scattering particles. Similarly the minimum will only appear in the regions of the parameter space where $\mu > m$ and $\lambda < 0$, i.e. region (a) of figure 2($A$), or $\lambda > 0$ and $\beta^2 < \lambda(\mu^2 - m^2)$, regions (d), (e) and (f ) of figure 2($A$). For $\mu < m$ the minimum will appear if $\lambda < 0$ and $\beta^2 > \lambda(\mu^2 - m^2)$, regions (g) and (h) of figure 2($B$). Figure 4 shows the shape of the reflection cross section in the different regions of the parameter space. Note the existence of the resonance peak in figures 4($A$), ($B$) and ($C$) and the zero cross section in 4($A$), after the resonance, 4($B$), before the resonance, and in 4($E$).

The shape of the cross section close to a narrow resonance peak is well approximated by the Breit–Wigner formula [18, 21]

$$\sigma_{\mathrm{tot}}(\rho) \propto \left((\omega_\rho - \omega_0)^2 + \tfrac{1}{4}\Gamma^2\right)^{-1}, \tag{45}$$

where $\omega_\rho$ is the energy of the reflecting particle, $\omega_0$ is the mass of the resonance particle and $\Gamma$ is the decay rate of the resonance. By comparing (45) and (44) close to the resonance peak we find that the energy of the resonance particle is equal to $\mu$, the natural frequency of the boundary oscillator. This suggests a new interpretation for the resonance peak, if we view the boundary terms in the Hamiltonian, (14), as describing a (0+1)-dimensional field rather than a mechanical system then particles of this field will have mass $\mu$. Such particles would be strongly confined to the boundary as they are only able to propagate in the domain of the

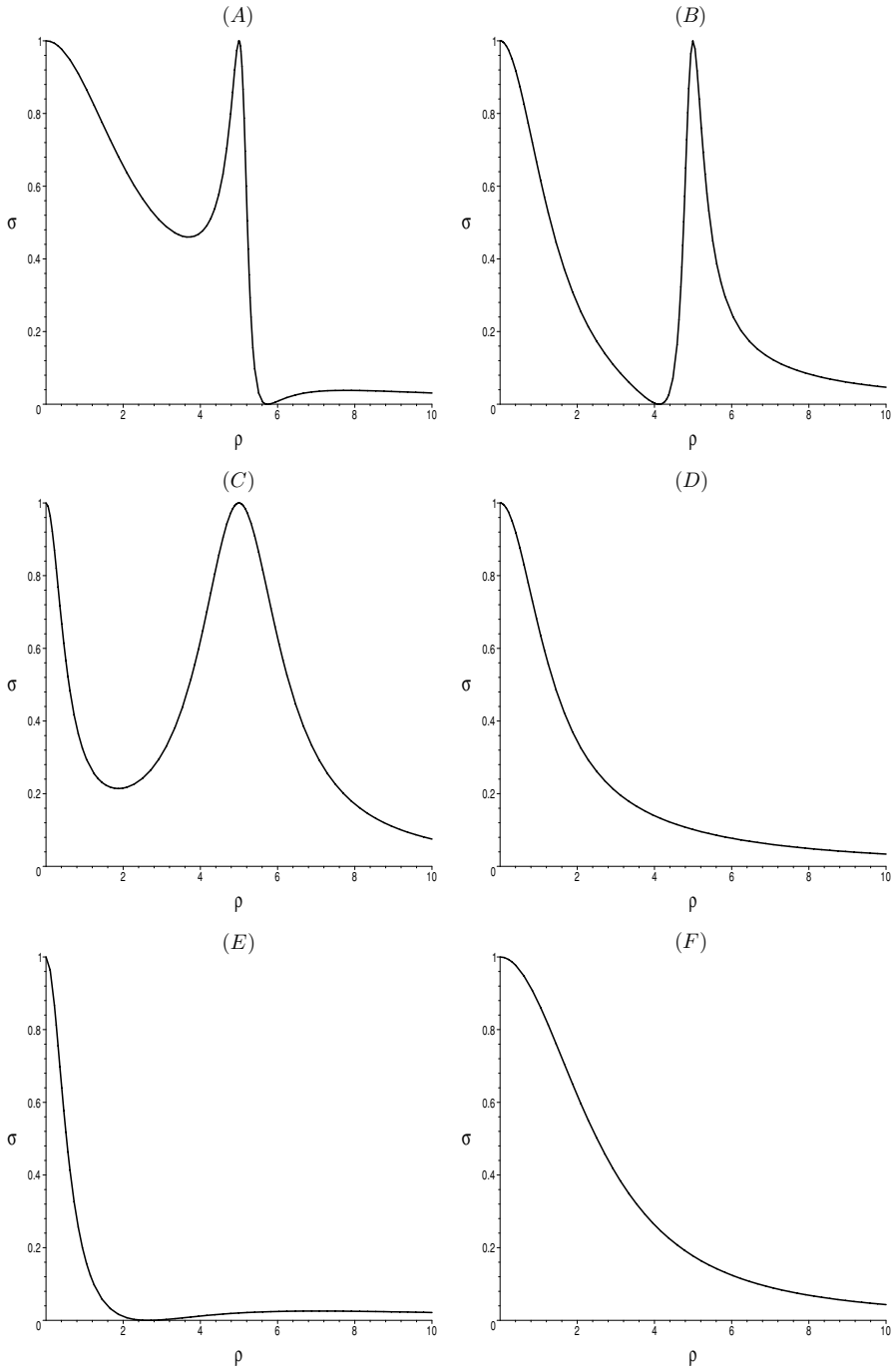


**Figure 4.** The total reflection cross section for the boundary oscillator with Robin potential for (*A*) $\lambda = -2,\ \mu = 13,\ m = 12,\ \beta = 4$, (*B*) $\lambda = 2,\ \mu = 13,\ m = 12,\ \beta = 4$, (*C*) $\lambda = 2,\ \mu = 13,\ m = 12,\ \beta = 8$, (*D*) $\lambda = -2,\ \mu = 12,\ m = 13,\ \beta = 4$, (*E*) $\lambda = -2,\ \mu = 12,\ m = 13,\ \beta = 8$, (*F*) $\lambda = 2,\ \mu = 12,\ m = 13,\ \beta = 4$.

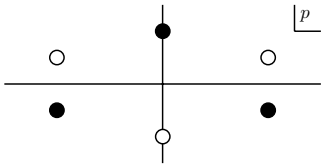


**Figure 5.** The analytic structure of the reflection matrix of the dynamic boundary with Robin potential for $\mu > m$ and $\lambda < 0$ (region (a)).

boundary field. The resonance peak corresponds to a bulk state, $|\rho\rangle$ with energy close to the mass, $\mu$, of the resonance state, $|\varsigma\rangle$, approaching the boundary and, through the linear coupling term, $\beta\phi(0,t)q(t)$, creates a boundary particle in state $|\varsigma\rangle$ which remains on the boundary until it decays back into the bulk state $|\rho\rangle$.

From (45) and (44) it is also possible to calculate an approximate value for $\Gamma$ which will be valid when the resonance is narrow,

$$\Gamma \approx \frac{\beta^2}{\mu\sqrt{\mu^2 - m^2}}. \tag{46}$$

As $\mu$ approaches $m$ the shape of the resonance peak widens corresponding to an increasing decay rate for the boundary particle. The Breit–Wigner formula (45) is only valid for narrow peaks so (46) ceases to be a good approximation.

Resonances associated with the boundary have been previously observed in [1, 14, 19, 20].

The zero reflection cross section arises from the combined effects of the boundary oscillator and the Robin boundary potential. A similar effect is observed in quantum mechanical scattering from a square well potential, see, for example, [22, 23]. Such minima in cross sections are often associated with the Ramsauer–Townsend effect where scattering of electrons from noble gas atoms show a minimum for certain energies of scattering electrons [24].

We will now turn our attention to the pole structure of the quantum reflection matrix (43), taking each of the regions of the parameter space in turn. In each case the reflection matrix has three poles corresponding to the three complex solutions of the cubic (26). First let us consider the region where $\mu > m$ and $\lambda < 0$, region (a) of figure 2(*A*). Figure 5 shows the analytic structure of the reflection matrix in this region, black circles denote poles and white circles denote nodes. In this case there in one pole on the positive imaginary axis and two in the lower complex half plane.

Earlier we observed a single classical boundary bound state solution when $\mu > m$ provided $\beta^2 > \lambda(\mu^2 - m^2)$. As $\beta^2$ and $(\mu^2 - m^2)$ are positive and $\lambda$ is negative there exists a boundary bound state in this region which corresponds to the pole on the positive imaginary axis in figure 5. Earlier in this section we observed that the reflection cross section in this region of the parameter space exhibits a resonance peak, as illustrated in figure 4(*A*). The unstable resonance state associated with this feature can be identified with the pole in the lower right quadrant of figure 5. The third pole in the lower left quadrant produces a resonance feature in the cross section at $\rho = -\sqrt{\mu^2 - m^2}$ however, as mentioned before, $\rho$ is a positive parameter so this resonance is never observed.

It is illuminating to consider how the poles behave in the weak coupling limit, i.e. as $\beta \to 0$ and $\lambda \to 0$ simultaneously. In this case the pole corresponding to the bound state approaches $\rho = 0$ along the positive imaginary axis. This indicates that the state arises from the stationary bulk particle state, the same behaviour as that of the bound state of the

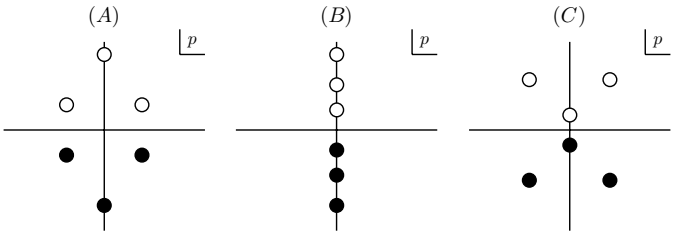


**Figure 6.** The analytic structure of the reflection matrix of the dynamic boundary with Robin potential for $\mu > m, \lambda > 0$ and (*A*) $\beta^2 < J_-$ (region (f)) (*B*) $J_- < \beta^2 < J_+ < \lambda(\mu^2 - m^2)$, or $J_- < \beta^2 < \lambda(\mu^2 - m^2) < J_+$ (region (e)), (*C*) $J_+ < \beta^2 < \lambda(\mu^2 - m^2)$ (region (d)).

attractive Robin boundary. Such states can be interpreted as particles of the field with energy less than their mass, $m$. These particles can only exist close to an attractive boundary. Thus the boundary in this region of the parameter space is attractive. The poles corresponding to the resonance states of the system in the weak coupling limit move onto the real $\rho$ axis at $\rho = \sqrt{\mu^2 - m^2}$. So when the coupling parameters are reduced the resonance state stabilizes with energy equal to the mass of the boundary field, $\mu$, as would be expected for a state which arises from the particle state of the boundary field.

We will now consider the region of the parameter space where $\mu > m, \lambda > 0$ and $\beta^2 < \lambda(\mu^2 - m^2)$, regions (d), (e) and (f). Figure 6 illustrates the possible configurations of the poles of the reflection matrix in these regions. In each case all three poles are located in the lower complex half plane, and at least one pole is located on the imaginary axis.

We know that there are no classical boundary bound state solutions in this region of the parameter space, poles located on the negative imaginary axis do not represent boundary bound states like those located on the positive imaginary axis. We also know that there is a resonance peak in this region. Let us consider the behaviour of the poles in the weak coupling limit[8], one pole approaches $\rho = 0$ along the negative imaginary axis, this is the same weak coupling behaviour displayed by the pole for the repulsive Robin boundary. Such poles do not carry a physical interpretation as a valid state of the system. Boundaries whose reflection matrix contains poles which have this weak coupling behaviour are repulsive to the particles of the field. The remaining poles of the reflection matrix approach $\rho = \pm\sqrt{\mu^2 - m^2}$ in the same way as described in the previous case. As before we can interpret one of these poles as being the resonance observed in figure 4(*B*), even though it may be located at purely imaginary values of $\rho$. Neither of the other poles of the reflection matrix have physical interpretations.

The third case we will consider is for $\mu > m, \lambda > 0$ and $\beta^2 > \lambda(\mu^2 - m^2)$, regions (b) and (c) of figure 2(*A*). Figure 7 shows the possible configurations of the poles of $R(\rho)$ in this region. Again we have a resonance as seen in figure 4(*C*) and we also have a classical bound state solution, which corresponds to the pole on the positive imaginary axis as usual. If we take the low coupling limit, ensuring $\beta^2 > \lambda(\mu^2 - m^2)$ remains valid, we find that this pole approaches $\rho = 0$ along the positive imaginary axis indicating that the boundary in this region is attractive. We can consider how the state behaves if we were to reduce $\beta^2$ and hold $\lambda$ constant (or increase $\lambda$ and hold $\beta$ constant). In this case the bound state pole passes through $\rho = 0$ when $\beta^2 = \lambda(\mu^2 - m^2)$. If $\beta^2$ is decreased further we will pass into a region of the parameter space where the boundary is repulsive. We know that this region does not have a

[8] Where $\lambda$ and $\beta$ are reduced such that $\beta^2 < \lambda(\mu^2 - m^2)$ is always true.

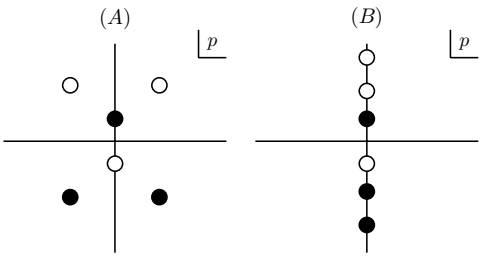


**Figure 7.** The analytic structure of the reflection matrix of the dynamic boundary with Robin potential for $\mu > m$, $\lambda > 0$ and (*A*) $\beta^2 > \lambda(\mu^2 - m^2) > J_+$, or $\beta^2 > J_+ > \lambda(\mu^2 - m^2)$ (region (b)), (*B*) $\lambda(\mu^2 - m^2) < \beta^2 < J_+$ (region (c)).

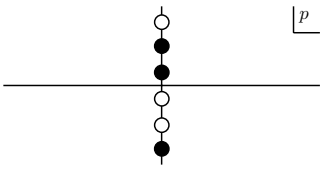


**Figure 8.** The analytic structure of the reflection matrix of the dynamic boundary with Robin potential for $\mu < m$, $\lambda < 0$ and $\beta^2 < \lambda(\mu^2 - m^2)$ (region (i)).

bound state, thus we conclude that the state corresponding to the bound state pole evaporates into a stationary bulk particle state as we make the transition between the two regions. The remaining poles behave in the low coupling limit in the same manner as described in the previous two cases and one is associated with the resonance state.

The fourth region we will consider is $\mu < m$, $\lambda < 0$ and $\beta^2 < \lambda(\mu^2 - m^2)$, region (i) of figure 2(*B*), we know that in this region there are two classical boundary bound state solutions, but there is no resonance state. Figure 8 shows the arrangement of poles of $R(\rho)$ for this region, as expected there are two poles on the positive imaginary axis corresponding to the two bound states.

In the weak coupling limit one of the bound state poles approaches $\rho = 0$ along the positive imaginary axis, indicating that this state is a boundary bound state in the sense of an attractive Robin boundary bound state, it arises from the stationary bulk particle state as the coupling is turned on. The presence of this state also indicates that the boundary is attractive in this region. The other poles behave differently in the weak coupling limit, they move towards the purely imaginary values, $\rho = \pm\sqrt{\mu^2 - m^2}$. The energy of these states becomes the same as the mass of the boundary field, $\mu$. Clearly these states arise from the particle state of the boundary field in the same manner as the resonances do when $\mu > m$. The pole on the positive imaginary axis is interpreted as the stable boundary state arising from the boundary field, the other pole lacks a physical interpretation.

The final parameter space regions we need to consider is when $\mu < m$, and $\beta^2 > \lambda(\mu^2 - m^2)$, which includes everywhere that $\lambda > 0$, the regions (g), (h), ( j) and (k) of figure 2(*B*). We know that in these regions there is a single classical boundary bound state and no resonance state. Figure 9 shows the possible analytic structure of the reflection matrix in these regions. In the weak coupling limit the pole on the positive imaginary axis moves to $\rho = \sqrt{\mu^2 - m^2}$, and carries the interpretation of being the state arising from the boundary particle state. A second pole approaches $\rho = 0$ along the negative imaginary axis, indicating that the boundary is repulsive.

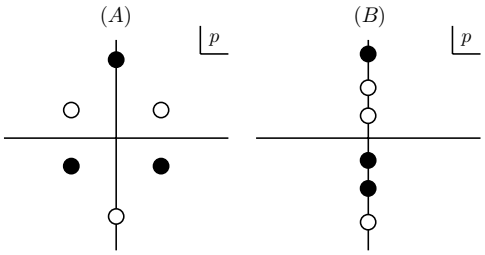


**Figure 9.** The analytic structure of the reflection matrix of the dynamic boundary with Robin potential for $\mu < m$ and (*A*) $\beta^2 > J_+$, (regions (g) and ( j)), and (*B*) $\lambda(\mu^2 - m^2) < \beta^2 < J_+$ (regions (h) and (k)).

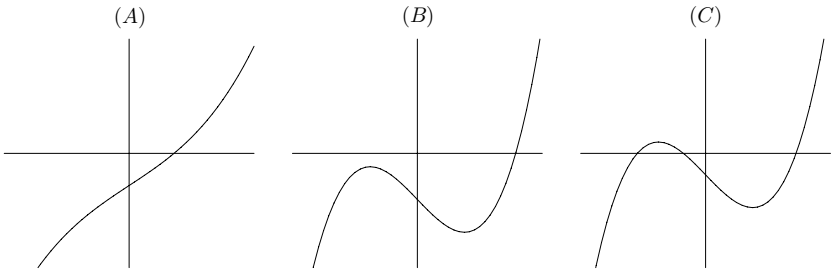


**Figure 10.** Graphs of the cubic $\varrho^3 + \varrho(\mu^2 - m^2) - \beta^2$ when (*A*) $\mu > m$, (*B*) $\mu < m$ and $\beta^2 > \frac{2}{27}(3(m^2 - \mu^2))^{3/2}$ and (*C*) $\mu < m$ and $\beta^2 < \frac{2}{27}(3(m^2 - \mu^2))^{3/2}$.

### *2.3. The* $\lambda = 0$ *special case*

In this section we will discuss a special case of the system considered previously where $\lambda = 0$ i.e. where the Robin boundary potential is removed leaving the field just coupled to the oscillator at the boundary.

Figure 10 shows the possible real solutions of (26) for $\lambda = 0$ and for different values of $m$, $\mu$ and $\beta$, clearly there is one and only one real positive solution for any allowed choice of the parameters. The condition on the parameters of the theory required for the bound state corresponding to this solution to be time oscillatory (and for the Hamiltonian to be bounded below) (27) becomes

$$\frac{\beta^2}{\mu^2} \leqslant m. \tag{47}$$

We note that when $m = 0$ equation (47) can only be satisfied by $\beta = 0$, i.e. a massless field in the bulk can only be coupled to a boundary oscillator in the presence of a (repulsive) Robin boundary potential.

In the quantized system the reflection matrix (43) simplifies to

$$R(p) = \frac{(p^2 - \mu^2 + m^2)p - \mathrm{i}\beta^2}{(p^2 - \mu^2 + m^2)p + \mathrm{i}\beta^2}. \tag{48}$$

The reflection matrix (48) has three poles, corresponding to the three complex roots of (26), one of these poles always occurs at positive, purely imaginary, values of momentum ($p = \mathrm{i}\varrho$) and corresponds to the classical bound state of the system, the features of which have been discussed previously. The remaining two poles occur at values of momentum in the lower half complex plane. To help interpret these poles we will initially assume that $\mu > m$, in which

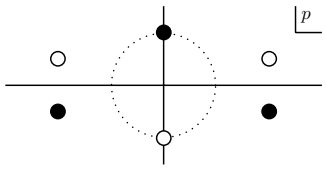


**Figure 11.** The analytic structure of the reflection matrix of the dynamic boundary for $\mu > m,\ \lambda = 0$.

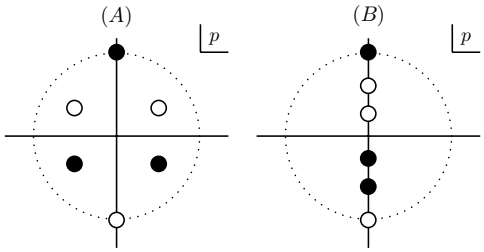


**Figure 12.** The analytic structure of the reflection matrix for the dynamic boundary for (*A*) $\mu < m$ and $\beta^2 > \frac{2}{27}(3(m^2-\mu^2))^{3/2}$ and (*B*) $\mu < m$ and $\beta^2 < \frac{2}{27}(3(m^2-\mu^2))^{3/2}$.

case the poles are arranged as shown in figure 11. The dotted circle describes the locus of points with the same modulus as the location of the bound state pole.

Figure 3(*A*) shows the shape of $\sigma_{\text{tot}}$ for the dynamic boundary in the region of the parameter space where $\mu > m$ and $\lambda = 0$. Figure 3(*A*) exhibits a resonance peak, the pole in the lower right quadrant of figure 11 corresponds to the resonance state.

We now have a full description of two of the poles of $R(p)$ in the region where $\mu > m$. The third pole of $R(p)$ carries a similar interpretation to that just presented for the resonance. If we were to continue figure 3(*A*) into negative values for $\rho$ we would observe a second resonance peak corresponding to the third pole of the reflection matrix. However, as mentioned before this region of the reflection matrix, and thus the cross section is never probed.

Before we conclude our discussion of this region of the parameter space let us consider the behaviour of the poles of the reflection matrix in the limit $\beta \to 0$, where the oscillator decouples from the field. From (48) we see that in this limit the pole corresponding to the bound state approaches $\varrho = 0$ from above. The energy of this state in the $\beta \to 0$ limit is equal to the mass of the bulk particle, $m$. This is the same behaviour as for the boundary bound state of the attractive Robin boundary potential in the limit $\lambda \to 0$ and indicates the bound state arises from the stationary bulk particle state. The ability for a boundary to support such a state indicates it is attractive to the particles of the field. In the limit $\beta \to 0$ the poles associated with the resonances stabilize and have energy equal to the mass of the particles of the boundary oscillator, $\mu$. This further supports the interpretation of the resonance particles as particles of the boundary field.

Let us now consider the region of the parameter space where $\mu < m$. Figure 12 shows the arrangement of poles and nodes of the reflection matrix in this region.

The reflection cross section can be calculated and plotted as previously, however, no additional features beyond background effects at low momentum are observed. To interpret these poles let us observe their behaviour as $\beta \to 0$. When $\mu < m$ we find that the bound state pole, being the one located at $p = \mathrm{i}\varrho$ on the positive imaginary axis, no longer goes to $\varrho = 0$ as the boundary coupling parameter is reduced. Instead its limiting energy is $\mu$, the

mass of the boundary particles. As in the previous case there is also a second pole which also has an energy $\mu$ in the weak coupling limit, but as it is located on the negative imaginary axis it carries no physical meaning. The final pole approaches $\varrho = 0$ from below as $\beta$ is reduced, this is the same behaviour as the pole in the reflection matrix of the repulsive Robin boundary. In both cases the pole does not correspond to any kind of bound state.

Clearly the spectrum of boundary states of the dynamic boundary is very different in these two regions of the parameter space. For $\mu > m$ there is a resonance state corresponding to the particles of the boundary field and a Robin-type boundary bound state arising from the attraction of the bulk particles to the boundary. However, when $\mu$ is reduced past $m$ the Robin-type bound state vanishes, just as for the Robin boundary when $\lambda$ is increased past zero. The resonance state becomes a new, stable, boundary bound state, classically this state can be thought of as the oscillator driving the field at the boundary but at a frequency too low to allow the energy to be dissipated away. The absence of a Robin-type boundary bound state suggests that the boundary oscillator in this region is repulsive to the particles of the field.

## 3. Conclusion

In this paper we considered the massive Klein–Gordon field coupled to a boundary oscillator, with and without an additional Robin boundary potential. We showed that these systems can be solved classically and that the classical solutions can be written as a superposition of independent modes of oscillation. We observed classical boundary bound state solutions in some regions of the parameter space, the requirement that these solutions be time oscillatory is seen to be the same as the requirement that the Hamiltonian is bounded below. We develop a condition relating the parameters of the theories which, when satisfied, ensures that bound state is oscillatory and thus that the system is physical.

Writing the classical solutions as superposition of independent modes allows the system to be quantized using canonical methods. The quantum reflection matrices for the boundaries are found from the two point function of the field. We observed several interesting features in the total cross section of the reflection process, including resonances and Ramsauer–Townsend effects. Although resonances associated with boundaries have previously been observed [1, 14, 19, 20] they have only previously been associated with boundaries containing additional degrees of freedom in [14]. Ramsauer–Townsend effects have not previously been observed in boundary field theories.

Quantum boundary bound states were observed in several regions of the parameter space. Some of these bound states were seen to arise from the states of the boundary oscillator, this behaviour has not previously been observed. Other boundary bound states arise in a similar manner to those of the attractive Robin boundary.

Similar systems to the ones described in this paper have previously been investigated. The coupling of one or more harmonic oscillators at fixed points in the bulk of a (1+1)-dimensional, massless, classical Klein–Gordon field is discussed in [10], and the coupling of a harmonic oscillator to a massless scalar field in a spherical reflecting cavity is discussed in [11, 12] where it is used to model the behaviour of an excited atom in a cavity. In [14] the massless scalar field coupled to a boundary oscillator is studied as a model of brane–bulk interaction in a braneworld universe. There also exist several papers dealing with quantum mechanical systems linked the some dissipative medium, based on the approach of [25] where the dissapative medium is modelled by coupling the system to an infinite number of harmonic oscillators. This modelling of the dispersive medium should be equivalent to the coupling of the system to the Klein–Gordon field, which contains an infinite number of harmonic oscillators, however, a correspondence between the results of this paper and those from

dissapative quantum mechanics has yet to be found. For a recent treatment of the harmonic oscillator using the methods of [25] see [26].

It seems that similar results to those presented in this paper should be obtainable for fields bounded by arbitrary linear mechanical systems. Of particular interest would be the existence and energy of boundary bound states and resonances for such systems. Other possibly interesting extensions include coupling two or more non-interacting bulk fields through a boundary or reformulating the present system to describe a point interaction on the whole line, or in a volume. In the latter case we would expect to make contact with the results of the earlier papers mentioned above.

## Acknowledgments

The author would like to thank Gustav Delius, Zoltàn Bajnok, László Palla, Gábor Takács, Evgeni Sklyanin and Bernard Kay for useful and interesting discussions. The author was supported by a PPARC studentship whilst undertaking this research.

## References

[1] Ghoshal S and Zamolodchikov A B 1994 Boundary S matrix and boundary state in two-dimensional integrable field theory *Int. J. Mod. Phys.* A **9** 3841 (*Preprint* hep-th/9306002)
Ghoshal S and Zamolodchikov A B 1994 **9** 4353(erratum)
[2] Sklyanin E K 1988 Boundary conditions for integrable quantum systems *J. Phys. A: Math. Gen.* **21** 2375
[3] Bajnok Z, Böhm G and Takács G 2004 On perturbative quantum field theory with boundary *Nucl. Phys.* B **682** 585 (*Preprint* hep-th/0309119)
[4] Bazhanov V, Lukyanov S and Zamolodchikov A 1999 On nonequalibrium states in QFT model with boundary interaction *Nucl. Phys.* B **546** 529 (*Preprint* hep-th/9812091)
[5] Baseilhac P and Delius G W 2001 Coupling integrable field theories to mechanical systems at the boundary *J. Phys. A: Math. Gen.* **34** 8259 (*Preprint* hep-th/0106275)
[6] Baseilhac P, Delius G W and George A 2002 Coupling the sine-Gordon field theory to a mechanical system at the boundary *Statistical Field Theories* ed A Cappelli and G Mussardo (Dordrecht: Kluwer) (*Preprint* nlin.SI/0201007)
[7] Baseilhac P and Kuizumi K 2003 Sine-Gordon field theory on the half-line with quantum boundary degrees of freedom *Nucl. Phys.* B **649** 491 (*Preprint* hep-th/0208005)
[8] Napomechie R 2001 The boundary supersymmetric sine-Gordon model revisited *Phys. Lett.* B **509** 183 (*Preprint* hep-th/0103029)
[9] Fuentes M, Lopez A, Fradkin E and Moreno E 1995 Bozonization rules in 1/2 + 1 dimensions *Nucl. Phys.* B **450** 603 (*Preprint* cond-mat/9502076)
[10] Chorosavin S A 2003 Simple exactly solvable models based on finite rank perturbation methods I: D'Alembert-Kirchhoff-like formulae *Preprint* maths.DS/0301137
Chorosavin S A 2003 Simple exactly solvable models based on finite rank perturbation methods II: resolvents formulae *Preprint* maths.DS/0301137
Chorosavin S A 2003 Simple exactly solvable models based on finite rank perturbation methods III: linear friction as radiation reaction *Preprint* math-ph/0307029
Chorosavin S A 2003 Simple exactly solvable models of one-dimensional scalar fields with concentrate factors *Preprint* math-ph/0311045
[11] Andion N P, Malbouisson A P C and Mattos Neto A 2001 An exact approach to the oscillation radiation problem in an arbitrary large cavity *J. Phys. A: Math. Gen.* **34** 3735 (*Preprint* physics/0001009)
[12] Flores-Hidalgo G, Malbouisson A P C and Milla Y W 2002 Stability of excited atoms in small cavities *Phys. Rev.* A **65** 063414
[13] Flores-Hidalgo G and Malbouisson A P C 2003 Time evolution of quantum systems in microcavities and in free space—a non-perturbative approach *Preprint* hep-th/0308198
[14] Binetruy P, Bucher M and Carvalho C 2004 Models of the brane–bulk interaction: toward understanding braneworld cosmological perturbation *Phys. Rev.* D **70** 043509 (*Preprint* hep-th/0403154)
[15] Fulling S A 1989 *Aspects of Quantum Field Theory in Curved Spacetimes* (Cambridge: Cambridge University Press)

[16] Bajnok Z, Böhm G and Takács G 2002 Boundary reduction formula *J. Phys. A: Math. Gen.* **35** 9333 (*Preprint* hep-th/0207079)
[17] Peskin M E and Schroder D V 1995 *An Introduction to Quantum Field Theory* (Reading, MA: Addison-Wesley)
[18] Weinberg S 1995 *The Quantum Theory of Fields* (Cambridge: Cambridge University Press)
[19] Mosconi P, Mussardo G and Riva V 2002 Boundary quantum field theories with infinite resonance states *Nucl. Phys.* B **621** 571 (*Preprint* hep-th/0107082)
[20] Bajnok Z, Palla L and Takács G 2002 The spectrum of boundary sine-Gordon theory *Preprint* hep-th/0211132
[21] Breit G and Wigner E P 1936 Capture of slow neutrons *Phys. Rev.* **49** 519
[22] Rae A I M 1992 *Quantum Mechanics* 3rd edn (Bristol: Institute of Physics Publishing)
[23] Greenhow R C 1990 *Introductory Quantum Mechanics* (Bristol: Institute of Physics Publishing)
[24] Holtsmark J 1929 Der ramsauereffekt im argon *Z. Phys.* **55** 437
[25] Caldeira A O and Leggett A J 1981 Influence of dissipation on quantum tunneling in macroscopic systems *Phys. Rev. Lett.* **46** 211
Caldeira A O and Leggett A J 1983 Quantum tunneling in dissipative systems *Ann. Phys.* **149** 374
[26] Rosenfelder R 2003 Structure function of a damped harmonic oscillator *Phys. Rev.* C **68** 034602 (*Preprint* nucl-th/0303003)